

We are IntechOpen, the world's leading publisher of Open Access books Built by scientists, for scientists

4,800

Open access books available

122,000

International authors and editors

135M

Downloads

Our authors are among the

154

Countries delivered to

TOP 1%

most cited scientists

12.2%

Contributors from top 500 universities



WEB OF SCIENCE™

Selection of our books indexed in the Book Citation Index
in Web of Science™ Core Collection (BKCI)

Interested in publishing with us?
Contact book.department@intechopen.com

Numbers displayed above are based on latest data collected.
For more information visit www.intechopen.com



Design and Analysis of SMA-Based Tendon for Marine Structures

Shahin Zareie and Abolghassem Zabihollah

Abstract

A tension-leg platform (TLP), as an offshore structure, is a vertically moored floating structure, connecting to tendon groups, fixed to subsea by foundations, to eliminate its vertical movements. TLPs are subjected to various non-deterministic loadings, including winds, currents, and ground motions, keeping the tendons under ongoing cyclic tensions. The powerful loads can affect the characteristics of tendons and cause permanent deformation. As a result of exceeding the strain beyond the elastic phase of the tendons, it makes unbalancing on the floated TLPs. Shape memory alloy (SMA)-based tendons due to their superelasticity properties may potentially resolve such problem in TLP structures. In the present work, performance and functionality of SMA wire, as the main component of SMA-based tendon under cyclic loading, have been experimentally investigated. It shows a significant enhancement in recovering large deformation and reduces the amount of permanent deformation.

Keywords: tension-leg platform, shape memory alloy, tendon, the superelasticity, cyclic load

1. Introduction

Marine and offshore structures are the key elements in energy supply chains in modern communities. A wide range of offshore structures including fixed and floated platforms, particularly tension-leg platform (TLP), are used to discover, extract, and transport the fossil fuel from seas and oceans.

According to the depth of the sea or oceans, proper offshore structures are chosen. For instance, for the depth between 300 and 1500 m, TLPs are the optimized platforms. TLPs are classes of floating offshore structures, fixed by a tendon to the seabed, as presented in **Figure 1** [2]. Tendons prevent vertical movements under tough external loadings from periodic, such as day-to-day winds and currents, to nonperiodic, like hurricanes and earthquakes [3–5]. Each of those loadings can put the integrity of the TLPs at risk.

In order to prevent any instability and damage, the applied loads should be prioritized with respect to the intensity. One of the most hazardous loadings is seismic activities, which can affect the integrity directly or indirectly by generating powerful loads, called the tsunamis. In TLPs, the seismic load's effect can be transferred by tendons to the main structures; hence, any damage or residual deformation in tendons makes the whole structure unbalanced and unstable.

In order to enhance the dynamic behavior of the tendons, the ideal tendons should be able to recover the original shape after experiencing large deformation

and be able to absorb the energy of seismic activities [6–10]. With respect to these desired outcomes, the shape memory alloy (SMA) is an ideal alternative to replace the conventional materials for making tendons, as shown in **Figure 2**.

An SMA is a class of smart materials with unique properties to return original shape by applying heat after removing the load, called shape memory effect (SME) or only removing loads, called superelasticity (SE). The SME and SE's state depends on the applied straining and working temperature. In both the SME and SE, the SMA is capable of dissipating the energy of the external loads. Overall, SMAs in the SE state are much popular than the SME mode, due to the simplicity of use and no need for any external source of heat. Nowadays, SMA-based applications are extensively used in many engineering applications, such as aerospace, automotive, civil infrastructure, and particularly, marine and offshore structures [6, 9–13].

The suggested SMA-based tendons are composed of SMA wires. The functionality of SMA wires under long-term cyclic loading is a crucial parameter to use for TLPs. In this study, the performance of the SMA wires is evaluated by exposing under cyclic loading.

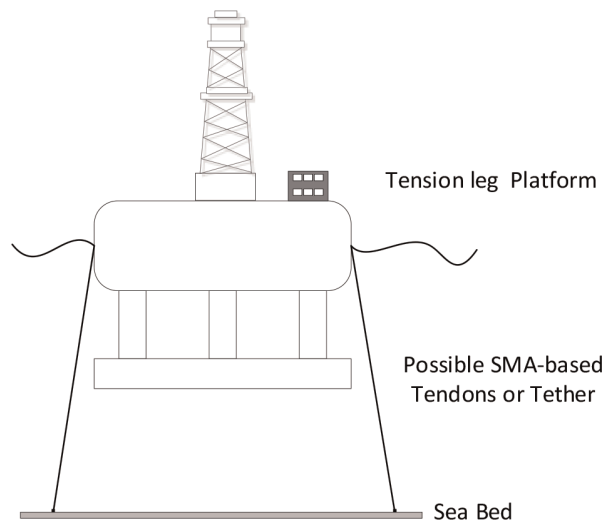


Figure 1.
The schematic diagram of TLP with SMA-based tendons taken from [1].

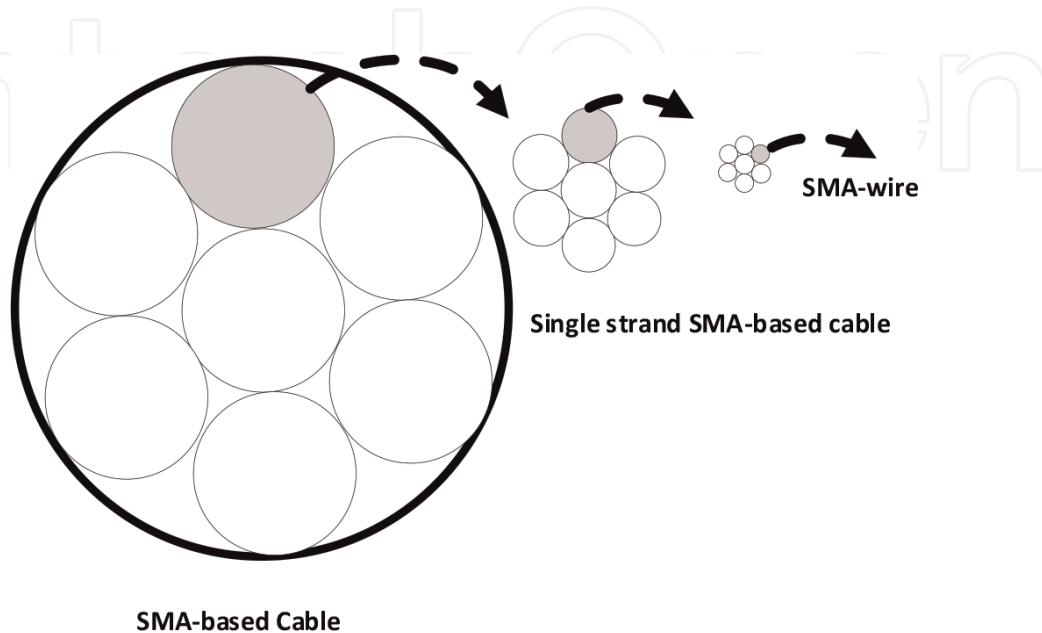


Figure 2.
The schematic diagram of the SMA-based tendon and its components taken from.

2. Shape memory alloy

The simplified constitutive law of superplastic SMA can be expressed by [14]:

$$\sigma(\varepsilon) = E(\varepsilon - \varepsilon^T) \quad (1)$$

where σ , E , ε , and ε^T are the stress, the Young modulus of SMA, the strain, and the phase transformation strain, respectively.

The Young modulus of SMA is given by [14]:

$$E = E_A + \zeta(E_M - E_A) \quad (2)$$

where ζ denotes the phase transformation volume fraction. E_M and E_A are the Young modulus in the Martensite phase and the Young modulus in the Austenite phase, as presented in **Figure 3**.

In the loading phase, ε^T is given by [14]:

$$\varepsilon^T = \zeta \varepsilon_L^T \quad (3)$$

In the unloading phase, ε^T is given by

$$\varepsilon^T = \zeta \varepsilon_{ULT} \quad (4)$$

In Eqs. (3) and (4), ε_L^T and ε_{ULT}^T denote the maximum phase transformation strain from Martensite to the Austenite and maximum phase transformation strain from Martensite to the Austenite from Austenite to Martensite, respectively.

The relation between ε_{ULT}^T and ε_L^T is expressed by [14]:

$$\varepsilon_{ULT}^T = \varepsilon_L^T + \frac{\sigma_{ms} - \sigma_{af}}{E_A} - \frac{\sigma_{mf} - \sigma_{as}}{E_M} \quad (5)$$

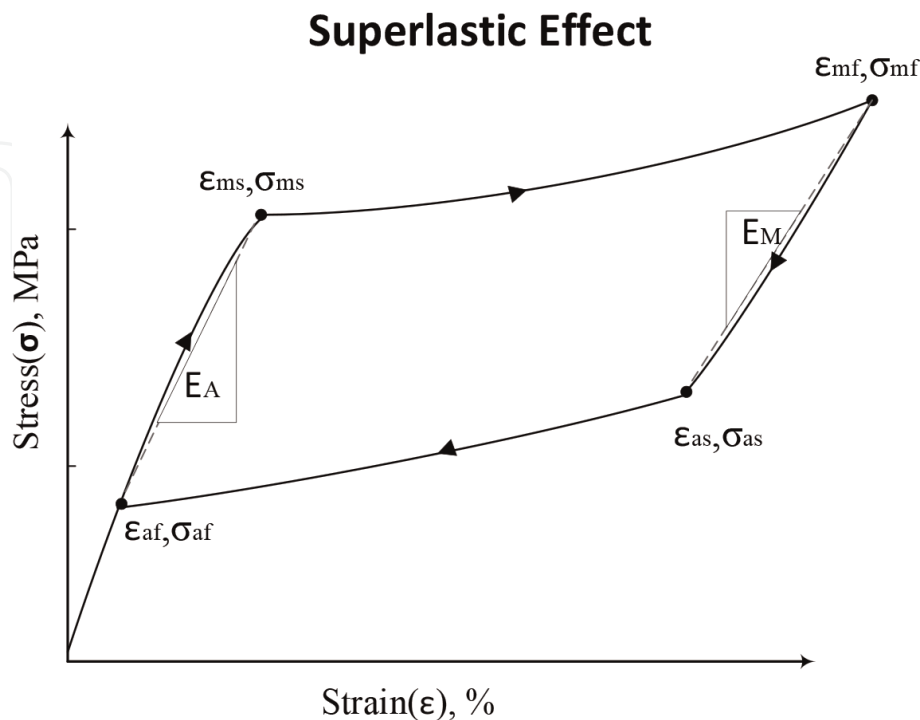


Figure 3.
 The schematic diagram of strain-stress behavior of the shape memory alloy.

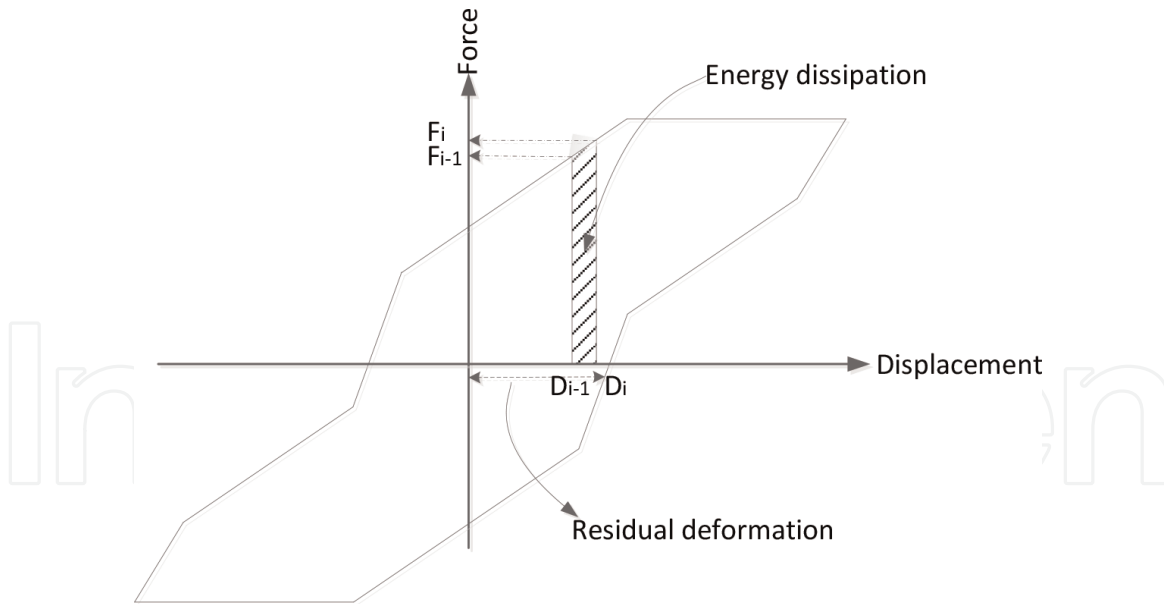


Figure 4.
The schematic diagram of the hysteresis response.

where σ_{ms} and σ_{mf} are the Martensite phase start stress to the Martensite phase finish stress, correspondingly. Similarly, σ_{as} and σ_{af} denote the Austenite phase start stress and Austenite phase finish stress. These stresses are displayed in **Figure 3**.

2.1 Energy dissipation

One of the main advantages of SMA tendon is the energy dissipation capacity. To compute this, the hysteresis response of the SMA is divided into elements, as shown in **Figure 4**. The energy dissipation of each element is expressed by

$$Energy_{total} = \sum_{i=1}^{n-1} 0.5(F_i + F_{i-1})(D_i - D_{i-1}) \quad (6)$$

where F_i and D_i stand the force and displacement of i -node in i -th element.

The total energy dissipation capacity of SMA is the sum of all energy dissipation capacity in each element.

3. Experimental configuration

In order to apply the dynamic cyclic load on the SMA wire, the MTS model 370.5 in the University of British Columbia, Okanagan Campus is used. It is a loading frame machine with an ability of 500 kN loading capacity. This machine is a programmable system equipped with sensor, actuators, control system, and software to run and collect data. This system and its accessories are displayed in **Figure 5**.

3.1 Shape memory alloy

Nowadays, among the different alloys for SMAs, nickel-titanium or Nitinol (NiTi) is one of the most common SMAs. In the present study, NiTi fabricated by Confluent Medical Technologies Company is used. The SMA specimen with

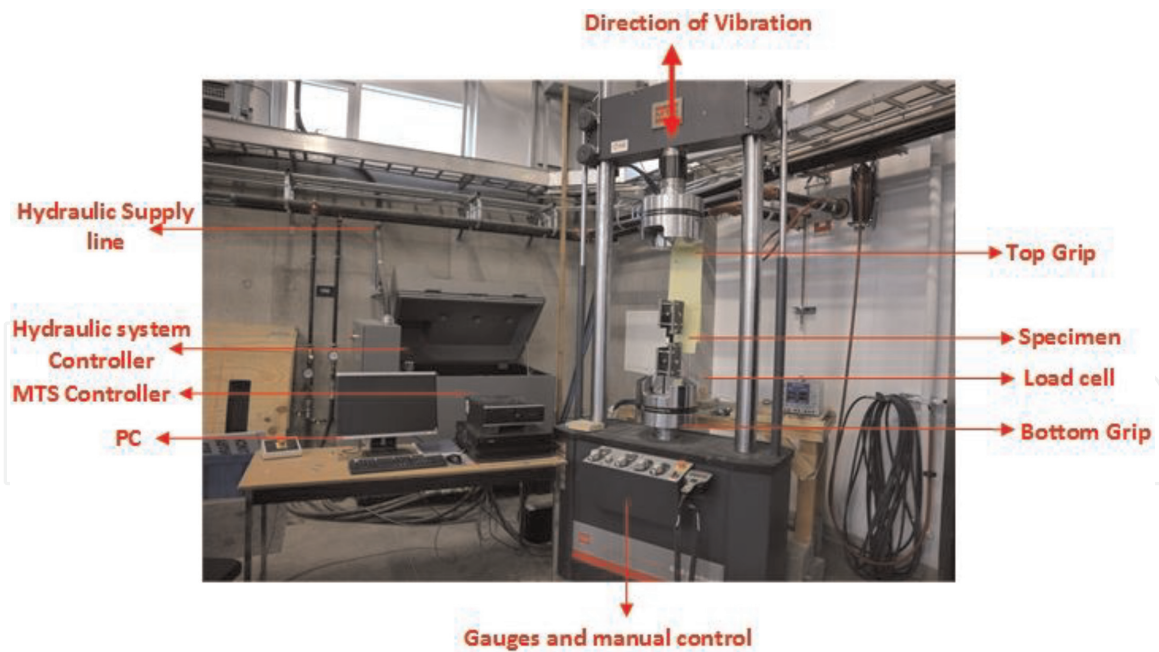


Figure 5.
 The MTS model 370.5 in the UBC and its accessories.

Physical properties	Value
Melting point (°C)	1310
Density (g/cm ³)	6.5
Modulus of elasticity (GPa)	41
Coefficient of thermal expansion (1/°C)	11×10^{-6}
Ultimate tensile strength (MPa)	~1070
Total elongation	~10%
Straight length (mm)	560
Radius (mm)	1.5

Table 1.
 The characteristics of NiTi shape memory alloy.

0.75 mm radius and 560 mm length is kept between the top and the bottom gripper of the MTS loading frame machine by two supportive steel plates. In order to perform the experimental tests, two specimens with 0 and 1.7% applied prestrained are used.

The mechanical properties are given in **Table 1**. It is observed that the density, the melting point, the coefficient of thermal expansion, the ultimate tensile strength, and the total elongation are 1310°C, 6.5 g/cm³, 41 GPa, ~1070 MPa, and ~10%, correspondingly.

4. Results

To simulate the effect of the long-term loading on the SMA specimens with and without applied prestraining, 1000 cyclic loads with the period of 1.4 s and the amplitude of 20 mm, as shown in **Figure 6**, are applied by the MTS loading frame machine.

The hysteresis responses of the SMA specimens are displayed in **Figure 7**. As seen, the strain-stress behavior of the SMA wires is a remarkable change under loading. It is found that the areas inside of hysteresis responses, representing energy dissipation capacities, decrease in both kinds of SMA specimens.

Another finding is the residual strain of the SMA specimen. It is noted that the residual strain of the SMA specimen without applying prestrained appears and changes up under cyclic loading. However, the prestrained SMA specimen is capable of fully recovering the original shape after exposing to the long-term cyclic loadings.

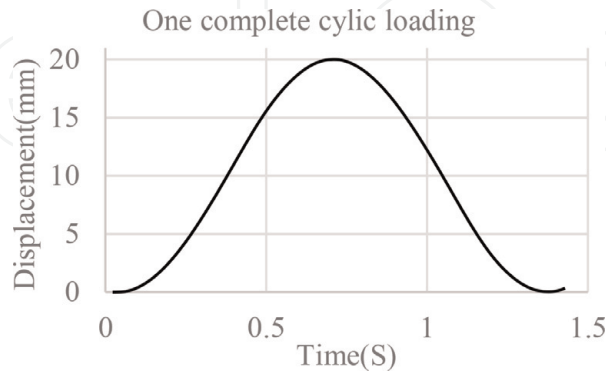


Figure 6.
1/1000 of applied cyclic loading by the MTS machine.

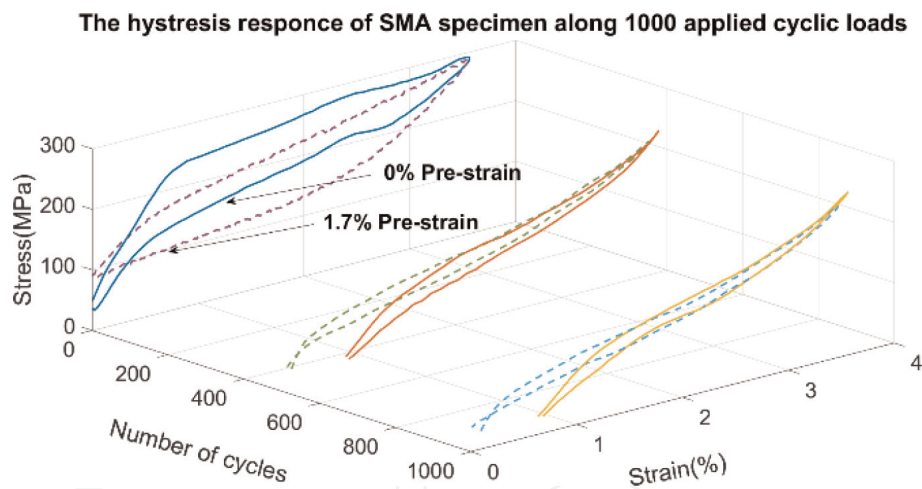


Figure 7.
Hysteresis response of the SMA along 1000 cyclic loadings.

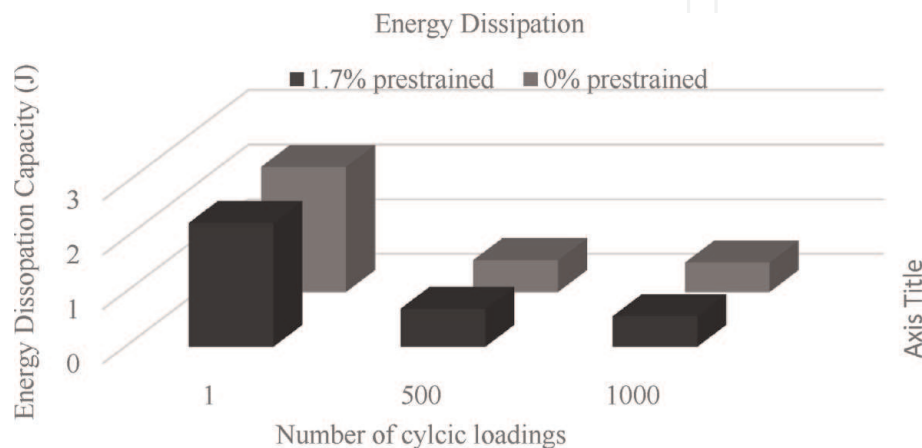


Figure 8.
The energy dissipation capacity of SMA specimens along 1000 cyclic loadings.

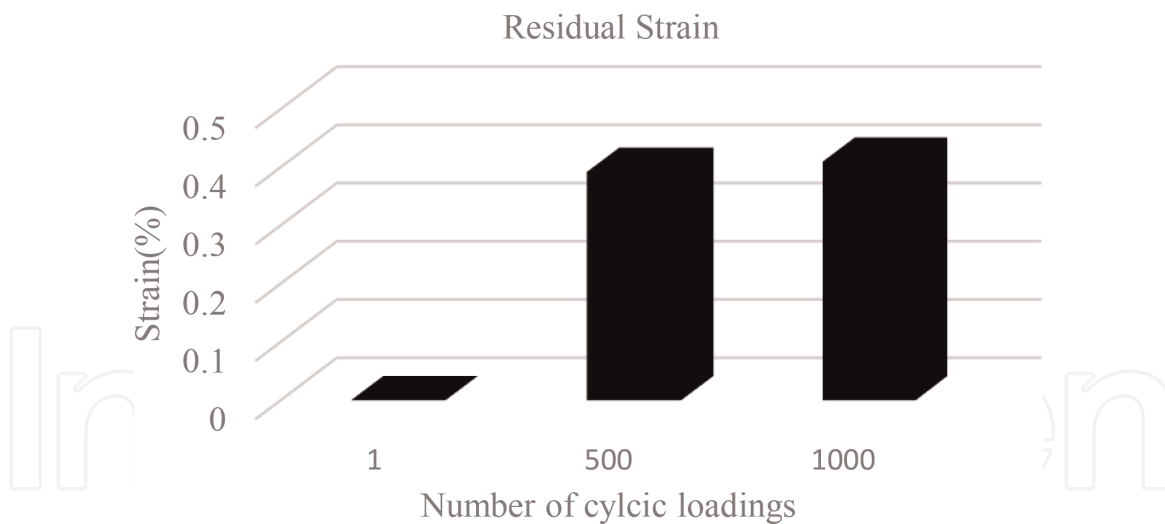


Figure 9.
The residual strain of the SMA specimen with 0% prestrained.

Figure 8 illustrates the contrast energy dissipation capacity between the SMA specimens. It is seen that the energy dissipation of the SMA without applied prestraining decreases significantly from 2.29 to 0.58 J after subjected 500 cyclic loadings and reaches 0.54 J after 1000 cyclic loadings. Under the same loading protocol, this amount in the SMA specimen with 1.7% prestrained reduces from 2.27 to 0.69 J exposed to 500 cyclic loadings and changes down to 0.56 J under 1000 cyclic loadings. This comparison shows that the rate of reduction in the energy absorption capacity of the 0% prestrained SMA wire in the first 500 cyclic is much more than the 1.7% prestrained SMA wire. Between 500 cycles and 1000 cycles, the similar drop in the energy absorption capacity in both specimens is observed.

The recovery ability is the next studied parameter in the 0% prestrained SMA specimen, as presented in **Figure 9**. Between 0-500 cyclic loading, the residual strain changes up from 0 to 2% strain of the initial strain and changes up to 3%. As seen, a remarkable drop in the recovery ability of the SMA in the first 500 cyclic loadings. In the last 500 cyclic loadings, the steady decrease in recovery ability is observed.

5. Conclusion

This study shows that the SMA-based tendon is an ideal alternative over the conventional tendon of TLPs. It can recover the original shape up to 4% of initial length. The effect of cyclic loading on SMA wires, as the main component of the SMA-based tendons of TLP, has been examined through experimental tests.

The main outcomes of the paper are as follows:

1. The SMA wire with and without applying prestrain can absorb the remarkable energy of external excitations. However, the degradation in SMA can decrease the energy dissipation capacity under long-term loadings. Hence, at least, the safety factor of the two should be determined due to the effect of the degradation in SMAs. It covers the reduction in that capacity during long-term loadings.
2. It is also suggested to consider the residual deformation while the system is designed; another solution is to apply the restraining. This action prevents to form any residual deformation in SMA-based tendon.

For the future study, the effect of a wide range of loading's frequencies and amplitudes on the performance of the SMA-based tendons is suggested.

Acknowledgements

This research received funding from the Green Construction Research and Training Center (GCRTC) and Desmond Schumann Memorial Award. The authors wish to thank the University of British Columbia, Okanagan Campus, for the technical support. The authors also wish to thank Mr. Kyle Charles as a research engineer and ex-manager lab for his valuable help in the experimental tests at the applied laboratory for advanced materials and structures at the University of British Columbia Okanagan Campus and M. Daghighi for the help received.

Author details


Shahin Zareie^{1*} and Abolghassem Zabihollah²

1 School of Engineering, The University of British Columbia, Kelowna, BC, Canada

2 School of Science and Engineering, Sharif University of Technology, International Campus, Kish Island, Iran

*Address all correspondence to: shahin@alumni.ubc.ca

IntechOpen

© 2020 The Author(s). Licensee IntechOpen. Distributed under the terms of the Creative Commons Attribution - NonCommercial 4.0 License (<https://creativecommons.org/licenses/by-nc/4.0/>), which permits use, distribution and reproduction for non-commercial purposes, provided the original is properly cited. 

References

- [1] Gagani A, Krauklis A, Echtermeyer AT. Anisotropic fluid diffusion in carbon fiber reinforced composite rods: Experimental, analytical and numerical study. *Marine Structures*. 2018;**59**:47-59
- [2] Bhaskara Rao DS, Panneer Selvam R. Response analysis of tension-based tension leg platform under irregular waves. *China Ocean Engineering*. 2016; **30**(4):603-614
- [3] Guo J, Wu J, Guo J, Jiang Z. A damage identification approach for offshore jacket platforms using partial modal results and artificial neural networks. *Applied Sciences*. 2018;**8**(11): 2173
- [4] Wang S, Li H, Han J, et al. Damage detection of an offshore jacket structure from partial modal information: Numerical study. In: *The Seventh ISOPE Pacific/Asia Offshore Mechanics Symposium*; 2006
- [5] Asgarian B, Aghaeidoost V, Shokrgozar HR. Damage detection of jacket type offshore platforms using rate of signal energy using wavelet packet transform. *Marine Structures*. 2016;**45**: 1-21
- [6] Zareie S, Mirzai N, Alam MS, Seethaler RJ. A dynamic analysis of a novel shape memory alloy-based bracing system. In: *CSCCE 2017*; 2017
- [7] Zareie S, Mirzai N, Alam MS, Seethaler RJ. An introduction and modeling of novel shape memory alloy-based bracing. In: *CSCCE 2017*; 2017
- [8] Aryan H, Ghassemieh M. A superelastic protective technique for mitigating the effects of vertical and horizontal seismic excitations on highway bridges. *Journal of Intelligent Material Systems and Structures*. 2017; **28**(12):1533-1552
- [9] Zareie S, Alam MS, Seethaler RJ, Zabihollah A. Effect of cyclic loads on SMA-based component of cable-stayed bridge. In: *7th International Specialty Conference on Engineering Mechanics and Materials*; 2019
- [10] Zareie S, Alam MS, Seethaler RJ, Zabihollah A. An experimental study of SMA wire for tendons of a tension leg platform. In: *5th Annual Engineering Graduate Symposium*; 2019
- [11] Zareie S, Alam MS, Seethaler RJ, Zabihollah A. Effect of shape memory alloy-magnetorheological fluid-based structural control system on the marine structure using nonlinear time-history analysis. *Applied Ocean Research*. Oct 1 2019;**91**:101836
- [12] Aryan H, Ghassemieh M. Mitigation of vertical and horizontal seismic excitations on bridges utilizing shape memory alloy system. *Advanced Materials Research*. 2014;**831**:90-94
- [13] Mirzai N, Attarnejad R. Performance of EBFs equipped with an innovative shape memory alloy damper. *Scientia Iranica*. 2018. DOI: 10.24200/sci.2018.50990.1955
- [14] Zuo X-B, Li A-Q, Sun X-H. Optimal design of shape memory alloy damper for cable vibration control. *Journal of Vibration and Control*. 2009;**15**(6): 897-921